REPORT DOCUMENTATION PAGE

Form Approved OMB NO. 0704-0188

1. REPORT DATE (DD-MM-YYYY)	2. REPORT TYPE	3. DATES COVERED (From - To)
28-12-2018	Final Report	1-Oct-2014 - 30-Sep-2018

4. TITLE AND SUBTITLE

Final Report: High Power, Single Frequency, Broad-area Diode Laser Emitters/Arrays and their Applications in Microresonator Based Frequency Combs - Optoelectronics program, ARO

5a. CONTRACT NUMBER
W911NF-14-1-0640

5b. GRANT NUMBER

5c. PROGRAM ELEMENT NUMBER
611102

6. AUTHORS

5d. PROJECT NUMBER

5e. TASK NUMBER

5f. WORK UNIT NUMBER

7. PERFORMING ORGANIZATION NAMES AND ADDRESSES

Clemson University
300 Brackett Hall
Box 345702
Clemson, SC 29634 -5702

8. PERFORMING ORGANIZATION REPORT NUMBER

9. SPONSORING/MONITORING AGENCY NAME(S) AND ADDRESS (ES)

U.S. Army Research Office
P.O. Box 12211
Research Triangle Park, NC 27709-2211

10. SPONSOR/MONITOR'S ACRONYM(S)
ARO

11. SPONSOR/MONITOR'S REPORT NUMBER(S)
66261-EL.13

12. DISTRIBUTION AVAILIBILITY STATEMENT

Approved for public release; distribution is unlimited.

13. SUPPLEMENTARY NOTES

The views, opinions and/or findings contained in this report are those of the author(s) and should not contrued as an official Department of the Army position, policy or decision, unless so designated by other documentation.

14. ABSTRACT

15. SUBJECT TERMS

16. SECURITY CLASSIFICATION OF:			17. LIMITATION OF ABSTRACT	15. NUMBER OF PAGES	19a. NAME OF RESPONSIBLE PERSON
a. REPORT	b. ABSTRACT	c. THIS PAGE			Lin Zhu
UU	UU	UU	UU		19b. TELEPHONE NUMBER 864-656-4381

RPPR Final Report
as of 09-Jan-2019

Agency Code:

Proposal Number: 66261EL **Agreement Number: W911NF-14-1-0640**
INVESTIGATOR(S):

Name: Lin Zhu
Email: zhu3@clemson.edu
Phone Number: 8646564381
Principal: Y

Organization: **Clemson University**
Address: 300 Brackett Hall, Clemson, SC 296345702
Country: USA
DUNS Number: 042629816 EIN: 576000254
Report Date: 31-Dec-2018 Date Received: 28-Dec-2018
Final Report for Period Beginning 01-Oct-2014 and Ending 30-Sep-2018
Title: High Power, Single Frequency, Broad-area Diode Laser Emitters/Arrays and their Applications in Microresonator Based Frequency Combs - Optoelectronics program, ARO
Begin Performance Period: 01-Oct-2014 **End Performance Period:** 30-Sep-2018
Report Term: 0-Other
Submitted By: Lin Zhu Email: zhu3@clemson.edu
Phone: (864) 656-4381
Distribution Statement: 1-Approved for public release; distribution is unlimited.

STEM Degrees: 3 **STEM Participants:** 6

Major Goals: Please see the attached report.

Accomplishments: Please see the attached report.

Training Opportunities: Please see the attached report.

Results Dissemination: Please see the attached report.

Honors and Awards: Please see the attached report.

Protocol Activity Status:

Technology Transfer: Nothing to Report

PARTICIPANTS:

Participant Type: PD/PI
Participant: Lin Zhu
Person Months Worked: 2.00 **Funding Support:**
Project Contribution:
International Collaboration:
International Travel:
National Academy Member: N
Other Collaborators:

Participant Type: Graduate Student (research assistant)
Participant: Yeyu Zhu
Person Months Worked: 6.00 **Funding Support:**
Project Contribution:
International Collaboration:
International Travel:

National Academy Member: N
Other Collaborators:

Participant Type: Graduate Student (research assistant)
Participant: Xiangfeng Chen
Person Months Worked: 6.00 **Funding Support:**
Project Contribution:
International Collaboration:
International Travel:
National Academy Member: N
Other Collaborators:

Participant Type: Graduate Student (research assistant)
Participant: Siwei Zeng
Person Months Worked: 1.00 **Funding Support:**
Project Contribution:
International Collaboration:
International Travel:
National Academy Member: N
Other Collaborators:

CONFERENCE PAPERS:

Publication Type: Conference Paper or Presentation **Publication Status:** 1-Published
Conference Name: CLEO: Science and Innovations
Date Received: 30-Aug-2018 Conference Date: 10-May-2018 Date Published:
Conference Location: San Jose, California
Paper Title: Narrow-linewidth, tunable external cavity diode lasers through hybrid integration of quantum-well/quantum-dot SOAs with Si3N4 microresonators
Authors: Yeyu Zhu, Siwei Zeng, Xiaolei Zhao, Yunsong Zhao, and Lin Zhu
Acknowledged Federal Support: **Y**

Publication Type: Conference Paper or Presentation **Publication Status:** 1-Published
Conference Name: CLEO: Science and Innovations
Date Received: 30-Aug-2018 Conference Date: 11-May-2017 Date Published:
Conference Location: San Jose, California
Paper Title: Coherent beam combining on silicon chip through hybrid integration
Authors: Yeyu Zhu, Yunsong Zhao, and Lin Zhu
Acknowledged Federal Support: **Y**

Publication Type: Conference Paper or Presentation **Publication Status:** 1-Published
Conference Name: 2016 IEEE Photonics Conference (IPC)
Date Received: 30-Aug-2018 Conference Date: 02-Oct-2016 Date Published:
Conference Location: Waikoloa, HI, USA
Paper Title: Integrated coherent combining of photonic crystal Bragg lasers with triangular lattice
Authors: Yunsong Zhao, Yeyu Zhu, and Lin Zhu
Acknowledged Federal Support: **Y**

RPPR Final Report
as of 09-Jan-2019

Publication Type: Conference Paper or Presentation **Publication Status:** 1-Published
Conference Name: 2016 IEEE Photonics Conference (IPC)
Date Received: 30-Aug-2018 Conference Date: 02-Oct-2016 Date Published:
Conference Location: Waikoloa, HI, USA
Paper Title: Hybrid integration for coherent laser beam combining on silicon photonics platform
Authors: yunsong zhao, yeyu zhu, and lin zhu
Acknowledged Federal Support: **Y**

Final Report: High power, single frequency, broad-area diode laser emitters/arrays and their applications in microresonator based frequency combs

Abstract: The objective of this project is to create a new class of high power, single frequency diode lasers in an integrated platform for emerging applications. We first focus on monolithic beam combining and use photonic crystal Bragg lasers as the building block to create monolithically coupled diode laser emitters and coherent arrays for high power, single frequency applications. This approach is innovative in that it simultaneously solves the most critical problems associated with beam control of high power diode laser arrays i.e., broad-area, single-transverse-mode emitters, single frequency operation, and monolithic beam combining. We then use hybrid photonic integration to realize coherent beam combing of diode lasers for high power, single frequency applications. In addition, we show that the proposed high power, single frequency sources are important for integrated nonlinear optics applications, such as microresonator based frequency comb generation.

INTRODUCTION

Monolithic and hybrid integration platforms are both important for photonic integrated circuits (PICs). It is desirable for the laser sources integrated in both platforms to provide high power and single frequency operation for many emerging applications. However, it is difficult to realize simultaneous high power and single frequency operation by using conventional semiconductor distributed feedback (DFB) lasers. Integrated coherent beam combining (CBC) is a promising solution to overcome this challenge. In this paper, coherently combined, integrated diode laser systems are experimentally demonstrated through both monolithic and hybrid CBC. For monolithic CBC of broad-area lasers in the InP platform, two single triangular-lattice photonic crystal (PC) Bragg lasers are combined. The measurement results show that the output power of the combined PC Bragg lasers is increased and the single frequency operation is maintained. As for the hybrid CBC, a chipscale coherently combined laser system is experimentally demonstrated in the InP-Si_3N_4 platform through the manipulation of optical feedback at different output ports of the coupled laser cavities. Coherent combining of two InP-based reflective semiconductor amplifiers are obtained by use of the cross-coupling provided by an adiabatic 3-dB coupler in silicon nitride, with a combining efficiency of ~92%.

Photonic integrated circuits (PICs), also known as planar lightwave circuits, are devices comprising a variety of photonic functional elements, such as lasers, detectors, modulators, filters, routers and nonlinear processing units, on a small chip [1]. PICs can significantly reduce the photonic system size, weight, operation power, and cost, and have attracted a lot of research interest since the late 1960s [2].

PICs have provided a foundation platform for cost-effective, high-performance solutions in a wide range of applications, such as optical communication systems, optical interconnects and free-space communication systems [3]. The performance of state of the art PICs is reaching a stage that can enable a whole new class of applications beyond telecom and datacom. In recent years, the emerging applications of PICs in LiDAR [4], microresonator based frequency comb [5], and photon pair generation [6] have aroused considerable interests. Single frequency, high power semiconductor diode lasers are key components for implementing these emerging applications in the photonic integrated platform. However, the conventional single frequency distributed feedback (DFB) semiconductor lasers are based on the narrow stripe waveguide structure that can only provide up to tens of milliwatts output power with a few MHz spectral linewidth [7], [8]. To scale up the output power, coherent beam combining (CBC) can be

used to overcome this limitation. However, the traditional CBC laser system either is only compatible with narrow strip, single mode diode lasers or requires optical fibers [9], [10] and free-space components such as lens [11], [12], external cavities [13] and diffraction gratings [14]. In order to address the challenge, we propose and demonstrate integrated chipscale CBC systems that are suitable for single frequency, high power operation without the need of fiber or free-space optical components.

PICs have been fabricated in different material systems, such as silicon, III-V semiconductors, dielectrics, polymers, and nonlinear crystal materials [15]. The dominant platforms for commercially-available PICs are the monolithic III-V semiconductors (gallium arsenide and indium phosphide) and silicon based material systems [16]. III-V semiconductors are well suitable for light generation and detection. In addition, both passive and active components can be integrated in the same substrate [17]. Silicon-based PICs have also become very popular due to their compatibility with mature CMOS technologies, low cost and high-volume processing [18]. Silicon based materials have desirable properties for passive components and modulators. The alternative to the monolithic platform is to employ a hybrid or heterogeneous platform that can take advantage of different material systems [19]. In such a hybrid system, active and passive components are fabricated respectively with different material systems. The outputs of the active and passive devices are optically coupled through mode matching or free-space optics [20]. Since both monolithic and hybrid photonic integration are important for future PICs, high power, single frequency semiconductor lasers are needed for both platforms. In this paper, we propose and demonstrate the integrated CBC system in the indium phosphide (InP) monolithic platform and indium phosphide-silicon nitride (InP-Si_3N_4) hybrid platform, respectively.

This report is organized as follows. In Section II, we experimentally demonstrate the CBC of the photonic crystal (PC) Bragg lasers with triangular lattice in the InP monolithic platform. Our approach can effectively scale up the output power and maintain the single frequency operation. In Section III, we experimentally demonstrate the CBC in the chipscale InP-Si_3N_4 hybrid platform through the mode selection mechanism induced by asymmetric mirror losses. We find that the additional loss does not compromise the performance of the coupled lasers due to the destructive interference at the lossy output port. We show that the hybrid CBC laser system has a combining efficiency of 92% with the single frequency output. In Section IV, we summarize our findings and results.

COHERENT COMBINING IN INP MONOLITHIC PLATFORM

Single frequency diode lasers in the InP monolithic platform are usually based on the DFB laser structures. In these structures, the single frequency operation is obtained through both transverse and longitudinal modal control, where a single-mode waveguide is used to define the transverse mode and a DFB grating is used to select a single longitudinal mode. To avoid the thermal-optic effects and other nonlinear effects, the width of the single mode waveguide is about 2~3 microns, which limits the total output power of conventional DFB lasers in the InP platform.

In order to obtain high power, single frequency diode lasers in the InP monolithic platform, a broad-area, large emitting aperture is used here to overcome catastrophic optical damage (COD) and help with heat dissipation. In addition, both the transverse and longitudinal modal control are also required in the broad-area laser diode to obtain the single frequency operation. PC Bragg laser is a good candidate satisfying the requirements [21]-[23].

For monolithic CBC of broad-area lasers in the InP platform, we have proposed and demonstrated a zigzag-like array design capable of coherently combining angled-grating broad-area lasers in our previous work [24]. However, since the angled grating provides the modal control only in the transverse direction,

the lasers usually operate with multiple longitudinal modes. To obtain the single frequency operation, PC Bragg lasers with two dimensional (2D) periodic structures are used here, instead of 1D angled-grating broad-area lasers. Figure 1 shows the schematic plot of the combined PC Bragg lasers. We use two PC Bragg lasers with triangular lattice tilting to the opposite directions and overlap them at one facet. The overlapped area defines the beam combining/coupling region. Unlike the conventional PC Bragg laser [25], [26], the triangular lattice is used instead of the rectangular lattice in this work because the triangular lattice provides the geometric symmetry required for laser combining, which is the key to realize the complete lattice overlap of the two single emitters at the coupling region. As shown in Fig. 1, we use the Bragg diffraction to realize the full modal control and beam combining at the same time.

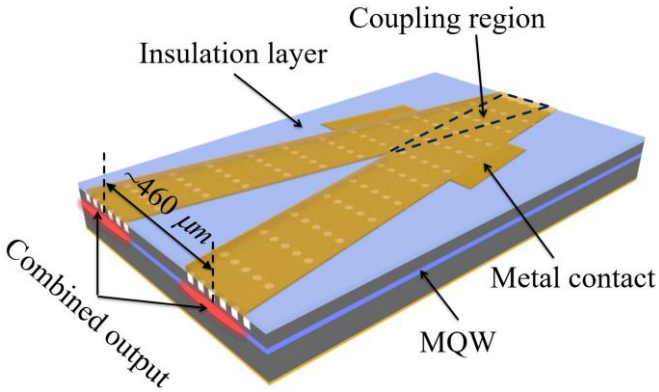

Fig. 1. Schematic plot of the integrated CBC system in the InP monolithic platform.

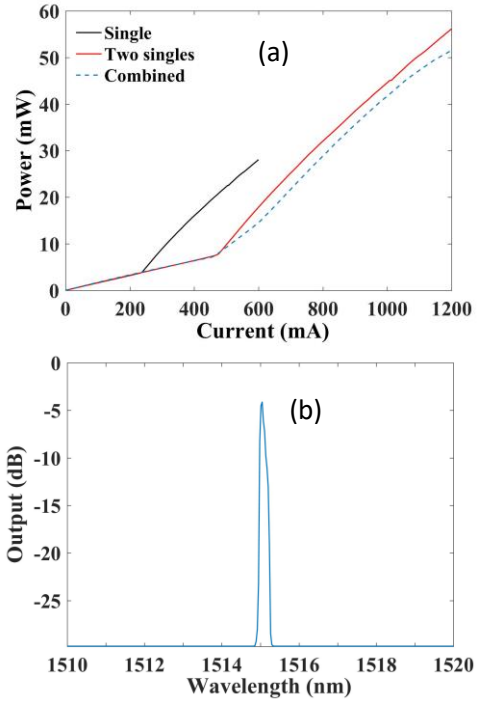

Fig. 2. L-I curves (a) and optical spectrum (b) of the combined PC Bragg lasers. The blue dashed line, black solid line and red solid line in (a) represent the L-I curves of the coherently combined PC Bragg lasers, single PC Bragg laser and two single PC Bragg lasers, respectively.

In Fig. 2(a), the LI curve of the coherently combined PC Bragg lasers with triangular lattice (blue

dashed line) shows that the threshold current is around 400 *mA* and the slope efficiency is about 0.14 *W/A*. Figure 2(a) also includes the LI curves of the single PC Bragg laser (black solid line) and the twice output power of the single PC Bragg laser (red solid line) for comparison. With a 100% power combining efficiency, the output power of the coupled emitters should be twice the output power of a single emitter when the injected current is doubled. Based on this rule, the measurement results in Fig. 2(a) show that the combining efficiency of the combined PC Bragg lasers is around 90%. The imperfect power combining efficiency is mainly caused by uneven power distribution of different emitters induced by the non-uniformity of the fabrication. Optimized etching, planarization and metallization processes can improve the fabrication uniformity. The optical spectrum is shown in Fig. 2(b), indicating the stable single frequency operation with a side mode suppression ratio larger than 25 *dB*. The pump current for this measurement is set at 1,000 *mA*.

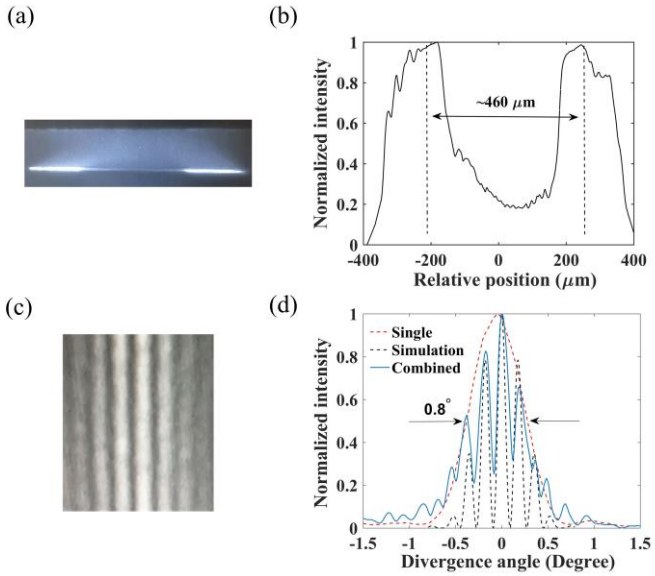

Fig. 3. The near field IR image (a), near field profile (b), far field IR image (c) and far field profiles (d) of the coherently combined PC Bragg lasers. The red dashed line, blue solid line and black dashed line in (d) represent the far field profiles of the uncoupled single PC Bragg laser, coherently combined PC Bragg lasers and simulation result, respectively.

Figure 3(a) and 3(b) present the near field infrared (IR) image and profile of the integrated CBC system. The center to center distance between the two emitting areas is ~ 460 μm and the width of each emitting area is ~ 110 μm. We can find that the light is indeed emitted from the designed emitters also shown in the schematic plot Fig. 1. Figure 3(c) and 3(d) show the far field IR image and profile of the integrated CBC system. The far field profile of the combined emitters is also compared with that of the individual single emitter. The uncoupled single emitter and coupled emitters were fabricated on the same chip with the same geometric parameters. Coherent beam combining of the two emitters will lead to constructive interference of the optical beams from the coupled emitters in the far field. In this case, the overall envelop of the interfered far field remains the same as that of the single emitter. The difference is that there would be interference fringes present within the overall envelop for the coupled emitters [24]. The expected far field profile is obtained in our measurement results shown in Fig. 3(c) and 3(d). The overall far field envelop of the combined PC Bragg lasers is very close to that of the individual single PC Bragg laser. The fine interference patterns in Fig. 3(c) and 3(d) prove that the two emitters are spatially coherent. The overall full width at half maximum (FWHM) divergence angles (~ 0.8°) are much smaller than a conventional broad-area laser (~ 10°) [27], [28]. The distance between the two emitting areas and the width of each emitting area are extracted from the measured near field profile in Fig. 3(b). The

theoretical far field pattern is calculated by using the standard diffraction theory with the assumption that the two combined emitters are in phase. The black dashed line in Fig. 3(d) shows the calculated far field profile. It agrees well with the measured result. The small difference in the divergence angles between the single emitter and the coupled emitters is mainly because the optical intensity distributions at the two emitting regions are slightly different for the coupled emitters [24].

The similar zigzag array design has been used in the previous work to coherently combine 1D angled-grating broad-area lasers [24]. However, the combined angled-grating broad-area lasers cannot provide the single frequency operation due to multiple longitudinal modes. In this paper, the 1D grating is replaced with the 2D triangular-lattice PC cavity. Since the mode control in both the transverse and longitudinal direction is provided in the PC cavity, we successfully obtain the single frequency operation. With the triangular lattice design, the coupling region shares the same lattice structure as the single emitter, which results in no interface mismatch between the combined emitters. This is important for obtaining uniform etching profile during fabrication and improving the device performance. Therefore, the monolithic CBC and single frequency operation can be realized simultaneously in the combined broad-area PC Bragg laser structures. The scalability analysis of this zigzag type of coherent combining can be found in Ref. [29]. Our results are important to realize the high power, single frequency semiconductor laser sources for PICs on a single chip by using the coherent beam combining of PC Bragg laser structures.

COHERENT COMBINING IN INP-Si_3N_4 HYBRID PLATFORM

Recently, silicon based materials (silicon, silicon oxide, and silicon nitride) have attracted a lot of attention for the PIC research [30]. Although silicon waveguides are good for providing tight optical confinement and large third order optical nonlinearity, they are not suitable for the applications that require high power CW light due to the two-photon absorption limiting the maximum light intensity. An alternative candidate, silicon nitride, has been used as a platform for integrated photonics to create passive optical components with high performance due to its low nonlinearity, high index contract with silica, very large transparency window and low linear propagation loss [31]. Another major challenge for Si/Si_3N_4 based PICs is to efficiently and reliably integrate electrically-pumped laser sources.

Hybrid integration has become a promising solution for multi-functional PICs beyond monolithic integration in recent years [32]-[35]. Such a hybrid system can create active and passive components on their native substrates with different material systems [36]-[40]. The outputs of the active and passive devices are optically coupled through mode matching or free-space optics [41]-[44]. A unique advantage associated with the hybridly integrated diode laser system is that the optical resonator and highly-absorbing active medium are separated, allowing for independent component optimization and better reliability. Besides, the Schawlow-Townes linewidth of the laser is greatly reduced due to the increased cavity photon lifetime [45], [46], which is obtained through increasing the effective cavity length and/or decreasing the cavity loss with the low loss PICs. The hybrid integration can be obtained through lens coupling, edge coupling, vertical coupling, die/wafer boning, or heteroepitaxy [47]. Until now the hybridly integrated diode lasers via edge-coupling exhibits the best performance [48] since the active chip and the passive chip can be optimized and fabricated independently. In this section, the CBC laser system in the InP-Si_3N_4 hybrid platform is experimentally demonstrated via edge-coupling. Our results are important for creating a hybridly integrated, high-power, single frequency laser source for passive PICs.

Figure 4(a) shows the schematic plot of the integrated CBC laser system based on the hybrid integration approach. In the CBC cavity design, two InP-based reflective semiconductor optical amplifiers (RSOAs) are connected by a 50:50 broadband directional coupler in a $Si_3N_4/SiO_2/Si$ chip. The coupling

efficiency between the gain chip and passive chip is improved through a mode converter on the passive chip. The RSOA has a high reflection (HR) coated back facet with 90% reflectivity and an anti-reflection (AR) coated front facet. The RSOA length is about 1 *mm*. The width and height of the single mode Si_3N_4 waveguide are 800 *nm* and 300 *nm*, respectively. The separation between the waveguides at the coupling region is 300 *nm*.

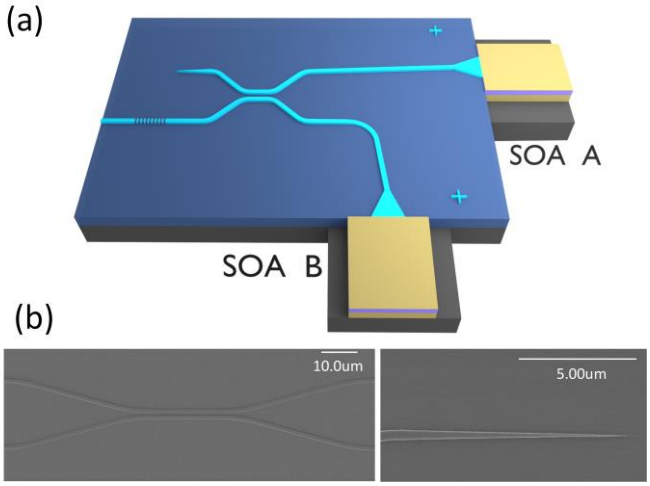

Fig. 4. (a) Schematic plot of the integrated CBC system in the InP-Si_3N_4 hybrid platform; (b) Scanning electron microscope images of the fabricated Si_3N_4 CBC cavity.

The two InP gain chips provide the optical gain for the hybrid laser cavity, whereas the adiabatic Si_3N_4 directional coupler on the silicon chip provides the intracavity coupling. The coupling results in the composite resonator modes (supermodes). The coupled cavities often support multiple supermodes and each supermode has a distinctive phase distribution among the gain elements [49], [50]. The supermode selection theory can explain the behavior of coherent combining and phase locking [9], [51]. If the coupled cavity consists of two identical cavities, both in-phase and out-of-phase supermodes will oscillate, and the output power should always be the same at both output ports. After the asymmetric mirror losses are introduced at the two output ports of the coupler, one of the supermodes with the lower modal loss will be selected, and the preferable single output is obtained. This means that the constructive interference occurs at the output port with the lower loss and the destructive interference occurs at the other output port with the higher loss. The differentiation between the supermodes results in the coherent combining of the two gain elements. Since it is easy to control passive optical components in the silicon based platform [52], the asymmetric mirror losses at the output ports are introduced in the passive chip. Here, we narrow down the waveguide width to zero for one output port of the coupler as shown in Fig. 4(a), which greatly enhances the mirror loss for this output port. The other output port provides optical feedback for lasing through a DBR reflector or cleaved facet. Figure 4(b) shows the scanning electron microscope images of the fabricated CBC cavity in the Si_3N_4 platform. The detailed fabrication processes can be found in Ref. [50].

To demonstrate the hybrid integration of two RSOAs and a passive chip, the active alignment is used here [50]. The RSOAs are kept at 23 °C by using thermo-electric coolers (TEC). Since the RSOA is directly coupled to the passive waveguide through butt coupling, the ridge waveguide in the RSOA gain chip and the Si_3N_4 waveguide are both angle-cleaved to suppress the reflection at the interface between the gain chip and the passive chip.

The coupling ratio of the coupler is 50:50

Figure 5(a) presents the schematic plot of the hybridly integrated, coherently combined laser system. We first only turn on one RSOA. The FDTD simulation result shown in Fig. 5(b) illustrates the power flow at the coupling region when only the RSOA at port 1 is turned on. At first, the light signal from port 1 is coupled into port 3 and 4 evenly. Then a broadband reflector at port 3 reflects the light back into the coupling region. Since the RSOA at port 2 is not turned on and port 4 is the lossy output port with almost no reflection, the light transmitted into port 4 and 2 is lost completely. The corresponding experimental results are illustrated in the top-view near field IR image of the passive chip in Fig. 5(d). The blue line area shows the lossy output port of the coupler, while the green line area shows the cleaved Si_3N_4 waveguide output facet. It is clear that the intensity of the scattered light inside the blue line area in Fig. 5(d) is strong, indicating high optical loss in this region. This result matches well with the FDTD simulation. Then, the two RSOAs are turned on simultaneously with the similar injection currents. The FDTD analysis in Fig. 5(c) shows that the light emitted from the two RSOAs will constructively interfere at port 3 and destructively interfere at port 4, if the two RSOAs are coherently combined and in-phase. This prediction matches well with our measurement results shown in Fig. 5(e). It is clear that the intensity of the scattered light near the lossy output port of the coupler is greatly suppressed (due to the destructive interference), while the output power obtained at the cleaved facet remains the same with the situation where only one RSOA is turned on. The ratio between the optical intensity near the lossy port in Fig. 5(d) and the one in Fig. 5(e) is ~9. Our measurement results prove that the two RSOAs are coherently combined by the hybrid CBC cavity.

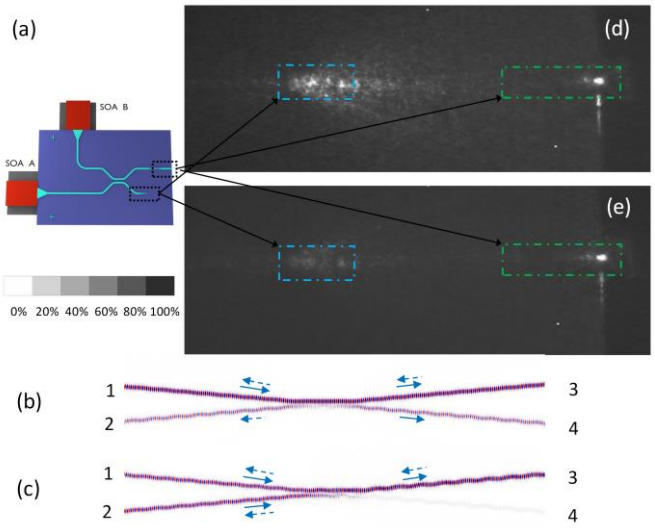

Fig. 5. (a) Schematic plot of the integrated CBC system in the InP-Si_3N_4 hybrid platform; FDTD simulation results and near field IR images (top-view) of the integrated CBC system if only RSOA B is turned on (b) and (d); RSOA A and B are turned on simultaneously (c) and (e). The grayscale bar shows the relative grey value.

Figure 6(a) shows the LI curves of the hybridly combined lasers and the single individual laser. For the single individual laser operation, we simply couple each RSOA with a single Si_3N_4 waveguide, where the same broadband reflector is used to provide the feedback. The corresponding LI curves are shown by the black and red line. For the hybridly combined lasers, both RSOAs are turned on simultaneously. The corresponding LI curve is shown by the blue line. Therefore, if the two lasers are coherently combined with a perfect combining efficiency, the output power of the combined lasers should be twice the output power of the single individual laser when the pump currents are the same.

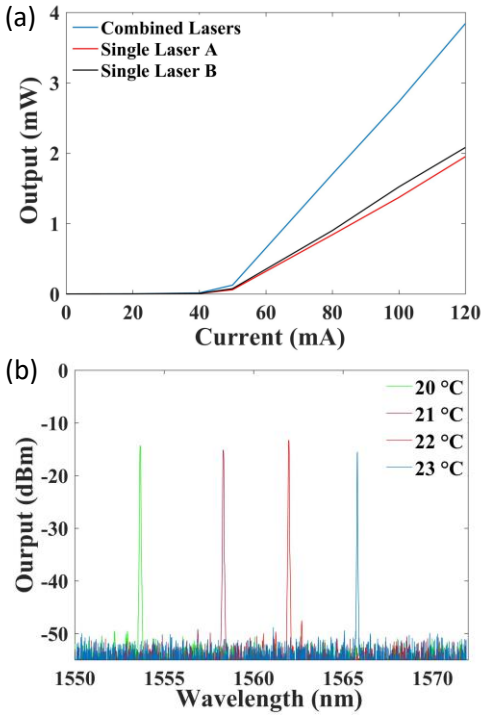

Fig. 6. LI curves (a) and optical spectra (b) of the hybridly integrated CBC system.

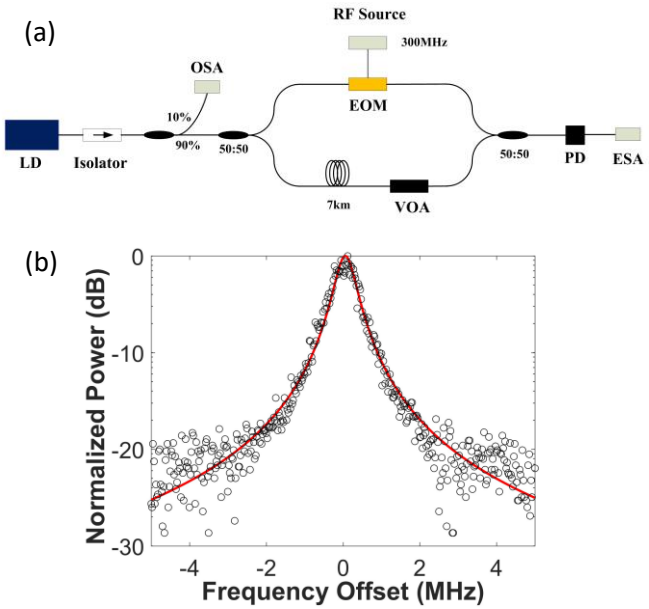

Fig. 7. (a) Delayed self-heterodyne experimental setup; OSA: optical spectrum analyzer; VOA: variable optical attenuator; PD: photodiode; ESA: electrical spectrum analyzer; EOM: electro-optic modulator; (b) Recorded beat spectrum (black circles), the red line shows a Lorentzian fit corresponding to a laser linewidth of 350-kHz.

As shown in Fig. 6(a), we obtain the combining efficiency of ~92% at I = 120 *mA* (~2× threshold). The measured high combining efficiency further proves that the two RSOA are indeed coherently combined. In addition, it should be mentioned that two RSOAs usually do not have the exactly same optical lengths. Thus, in our experiments, we first use the same injection currents for each RSOA to obtain the similar

optical gains in each laser cavity. Then, we slightly tune the injection current in one of the two RSOAs in order to obtain the optimal combining efficiency. The current tuning helps to find the common resonant mode and increase the combining efficiency. But the injection current difference between the two RSOAs to achieve the best combining efficiency is always small. Figure 6(b) shows the optical spectra for the combined lasers at different TEC temperatures. The pump currents are set at 100 *mA*. As we tune the temperature of the TEC, the lasing wavelengths change from 1554 *nm* to 1566 *nm*. At different temperatures, the single frequency operation is obtained with a side mode suppression ration higher than 30dB. The demonstrated wavelength tuning range is ~12 *nm*.

Since the optical spectrum analyzer does not have the adequate resolution to resolve the laser spectral linewidth, a delayed self-heterodyne (DSH) interferometer with a 7-km delay line is used to measure the spectral linewidth of the laser as shown in Fig. 7(a). Compared with the optical heterodyne detection approach, the DSH method does not need a reference laser with a narrower linewidth at a nearby frequency [53]. The measured RF-beat spectrum is shown as the black circles in Fig. 7(d). The red line shows a Lorentzian fit with a 3-dB bandwidth of 700-kHz, which corresponds to a 350-kHz FWHM laser linewidth. The measured linewidth compares favorably with the approximate 1-MHz linewidth of typical monolithic DBR and DFB laser sources [54], [55]. The linewidth of the hybrid laser is reduced mainly due to the increased cavity length. The linewidth can be further reduced by use of a microring based delay-line filter in the passive chip.

The coupling ratio of the coupler is 60:40

In this part, we investigate the performance of the hybrid laser if the coherent coupler does not have a desired 50:50 coupling ratio. This is important for evaluating the system robustness of the proposed hybrid CBC against fabrication errors. Here, we intentionally set the coupling ratio of the coupler to be around 60:40. Figure 8(a) shows the power flow in our system through FDTD analysis. The input light signal at port 1 is unevenly coupled into port 3 and port 4. The output power ratio between the port 3 and the port 4 is 60:40 since no reflection is used in the simulation.

The schematic plot of the hybridly integrated CBC laser system is the same as the one shown in Fig. 4 and Fig. 5(a), except that the coupling ratio of the coupler is set to be 60:40. Figure 8(b) shows the measured top-view near field IR image. When only one RSOA (i.e., RSOA B) is turned on, intense scattered light is observed near the blue line area. The blue line area corresponds to the lossy output port of the coupler, while the green line area still corresponds to the cleaved Si_3N_4 waveguide output facet.

Then, the two RSOAs are turned on at the same time. If the two RSOAs are coherently combined with a 100% efficiency, complete destructive interference must happen at port 4 as shown in Fig. 8(c). That means that the input power ratio between port 1 and port 2 should be around 60:40. Thus, the injection currents for the two RSOAs need to be different. In our experiment, the injection current for RSOA B is set to be around 80 *mA*, whereas the one for RSOA A is set to be around 70 *mA*. We select these values based on the measurement results of the single individual hybrid laser. From Fig. 6(a), we can find that the ratio of the output power between the single individual laser A (at 70 *mA*) and the single individual laser B (at 80 *mA*) is around 40:60. With these settings, we obtain the near field IR image shown in Fig. 8(d). It is clear that the intensity of the scattered light from the lossy output port of the coupler is greatly reduced (indicating destructive interference at port 4), while the output power obtained at the cleaved facet remains the same with the situation where only RSOA B is turned on. The results in Fig. 8 demonstrate that the two RSOAs are still coherently combined with a high efficiency through the passive CBC cavity with an asymmetric coupler.

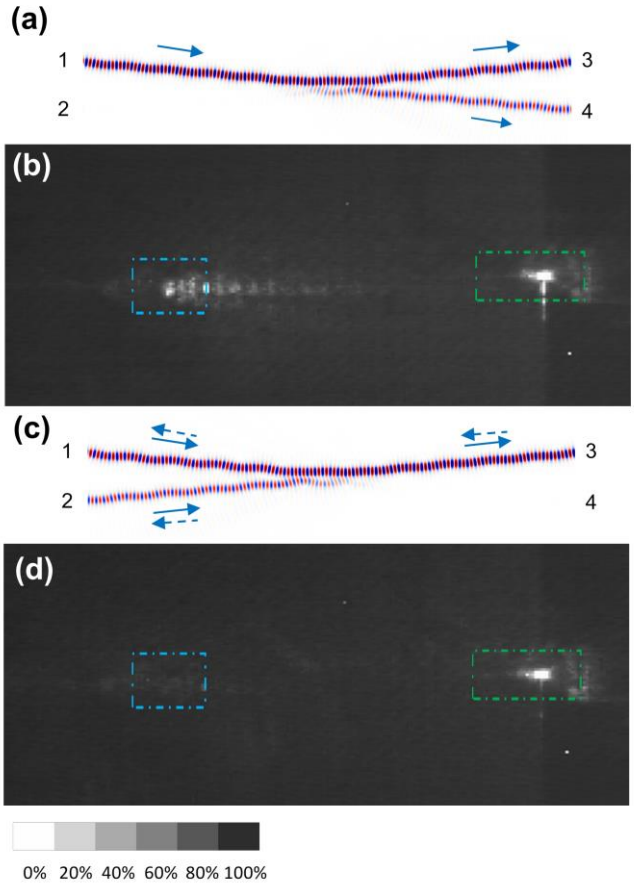

Fig. 8. (a) FDTD simulation results for the power flow at the coupling region, the coupling ratio is 60:40; (b) near field IR images (top-view) of the coherently combined lasers if only one RSOA is turned on; (c) FDTD simulation results and (d) near field IR images (top-view) of the coherently combined lasers if both two RSOAs are turned on at the same time. The grayscale bar shows the relative grey value.

In the traditional evanescently-coupled laser array, the modal discrimination among different supermodes is small. In order to obtain the efficient and robust single-mode operation, the modal discrimination has to be increased. In this paper, by introducing the asymmetric mirror losses into the coupled cavities, we improve the modal discrimination in the coherent array and obtain the efficient coherent combining and single frequency operation. The hybridly integrated CBC laser system can be used to create on-chip high power laser sources for integrated nonlinear optics applications on a single silicon chip. The hybrid integration scheme also allows for integrating other optical components on the same passive chip.

CONCLUSION

Integrated coherently combined laser system is a promising candidate for the realization of high power, single frequency laser sources for PICs. In this ARO project, chip-scale CBC laser systems have been successfully demonstrated in both InP monolithic platform and InP-Si_3N_4 hybrid platform for high power, single frequency applications. For the InP-based monolithic platform, the coherent beam combining of two PC Bragg lasers with triangular lattice is demonstrated. Our experimental results show that this method can be used to improve the laser output power and maintain the single frequency operation at the same time. The demonstrated combining efficiency is around 90%.

Furthermore, an integrated coherently combined laser system is demonstrated in the InP-Si_3N_4 hybrid

platform. Two InP-based gain chips are coherently combined via a Si_3N_4 directional coupler on the passive chip. Coherent combining is achieved by use of the intracavity optical coupling and asymmetric mirror losses for the coupled laser cavities. The measurement results show that the combining efficiency of our system is ~92% at ~2× threshold. The linewidth, wavelength tunability, and coupling ratio tolerance of the hybridly combined lasers are also investigated. The diode laser based chip-scale CBC systems have the desired system compactness by removing the need of bulk components and can provide the high power, single frequency operation for many emerging integrated photonics applications.

Education and outreach activities

We have trained three graduate students and three undergraduate students through this project. One graduate student and two undergraduate students obtained their degrees during the project period. We have published 12 journal and conference papers for this project.

Interdisciplinary research experience: Our research is interdisciplinary in nature as it requires the understanding of material science, optical physics, nanofabrication, and optical characterization. Therefore, through this project, undergraduate and graduate students have opportunities to learn about many aspects of laser systems and to interact with researchers from numerous disciplines.

Creative Inquiry to promote undergraduate research: The campus-wide initiative program, Creative Inquiry (CI), seeks to provide Clemson undergraduate students with creative inquiry experiences in an active research-oriented environment normally unavailable at the undergraduate level. The CI program gives participants more "real world" learning experience that promotes their intellectual, creative, reasoning, communicative, and critical thinking capabilities, thus creating a more effective environment for learning. Students take on team-based projects that cover interesting topics and allow them work with a group of peers and faculty mentors on three to four semesters basis. We have hosted three CI teams during the project period.

Clemson ECE Department Student Poster Competition: All ECE faculty, graduate, and undergraduate students engaged in research were invited to participate in this competition. The purpose of the ECE poster competition is to provide students and faculty the chance to showcase their research, and to provide high-quality visuals for those walking the halls of Riggs. We have used the results obtained in this project to participate the competition.

REFERENCES

[1] L. A. Coldren, S. W. Corzine, and M. L. Mashanovitch, "Diode lasers and photonic integrated circuits," 2nd ed., vol. 218, John Wiley & Sons, 2012.

[2] S. E. Miller, "Integrated optics: An introduction," *Bell Labs Technical Journal*., vol. 48, no. 7, pp. 2059-2069, 1969.

[3] L. A. Coldren, S. C. Nicholes, L. Johansson, S. Ristic, R. S. Guzzon, E. J. Norberg, and U. Krishnamachari, "High performance InP-based photonic ICs—A tutorial," *J. Lightw. Technol*., vol. 29, no. 4, pp. 554-570, 2011.

[4] E. Dale, W. Liang, D. Eliyahu, A. Savchenkov, V. Ilchenko, A. B. Matsko, D. Seidel, and L. Maleki, "Ultra-Narrow Line Tunable Semiconductor Lasers for Coherent LIDAR Applications," in Imaging and Applied Optics 2014, Optical Society of America, pp. JTu2C-3., 2014.

[5] P. Del'Haye, A. Schliesser, O. Arcizet, T. Wilken, R. Holzwarth, and T. J. Kippenberg, "Optical frequency comb generation from a monolithic microresonator," *Nature*, vol. 450, no. 7173, pp. 1214-1217, 2007.

[6] S. Clemmen, K. P. Huy, W. Bogaerts, R. G. Baets, P. Emplit, and S. Massar, "Continuous wave photon pair generation in silicon-on-insulator waveguides and ring resonators," *Opt. Express*, vol. 17, no. 19, pp. 16558-16570, 2009.

[7] L. M. Miller, J. T. Verdeyen, J. J. Coleman, R. P. Bryan, J. J. Alwan, K. J. Beernink, J. S. Hughes, and T. M. Cockerill, "A distributed feedback ridge waveguide quantum well heterostructure laser," *IEEE Photon. Tech. Lett.*, vol. 3, no. 1, pp. 6-8, 1991.

[8] M. Ziegler, J. W. Tomm, U. Zeimer, and T. Elsaesser, "Imaging Catas- trophic Optical Mirror Damage in High-Power Diode Lasers," *J. Elec. Mater*., vol. 39, no. 6, pp. 709-714, 2010.

[9] A. Shirakawa, T. Saitou, T. Sekiguchi, and K. I. Ueda, "Coherent addition of fiber lasers by use of a fiber coupler," *Opt. Express*, vol. 10, no. 21, pp. 1167-1172, 2002.

[10] T. W. Wu, W. Z. Chang, A. Galvanauskas, and H. G. Winful, "Model for passive coherent beam combining in fiber laser arrays," *Opt. Express*, vol. 17, pp. 19509-19518, 2009).

[11] C. J. Corcoran, and F. Durville, "Experimental demonstration of a phase-locked laser array using a self-Fourier cavity," *Appl. Phys. Lett*., vol. 86, no. 20, pp. 201118, 2005.

[12] C. Chang-Hasnain, D. F. Welch, D. R. Scifres, J. R. Whinnery, A. Dienes, and R. D. Burnham, "Diffraction-limited emission from a diode laser array in an apertured graded-index lens external cavity," *Appl. Phys. Lett*., vol. 49, pp. 614–616, 1986.

[13] B. Liu, Y. Liu, and Y. Braiman, "Coherent beam combining of high power broad-area laser diode array with a closed-V-shape external Talbot cavity," *Opt. Express*, vol. 18, pp. 7361–7368, 2010.

[14] O. Andrusyak, V. Smirnov, G. Venus, V. Rotar, and L. Glebov, "Spectral combining and coherent coupling of lasers by volume Bragg gratings," *IEEE J. Sel. Top. Quantum Electron*., vol. 15, no. 2, pp. 344-353, 2009.

[15] D. Liang, and J. E. Bowers, "Photonic integration: Si or InP substrates," *Electron. Lett*., vol. 45, no. 12, pp. 578-581, 2009.

[16] R. Nagarajan, M. Kato, J. Pleumeekers, P. Evans, S. Corzine, S. Hurtt, A. Dentai, S. Murthy, M. Missey, R. Muthiah, and R. A. Salvatore, "InP photonic integrated circuits," *IEEE J. Sel. Top. Quantum Electron.*, vol. 16, no. 5, pp.1113-1125, 2010.

[17] T. L. Koch, and U. Koren, "Semiconductor photonic integrated circuits," *IEEE J. Quantum Electron*., vol. 27, no. 3, pp. 641-653, 1991.

[18] P. Dong, X. Liu, S. Chandrasekhar, L. L. Buhl, R. Aroca, and Y. K. Chen, "Monolithic silicon photonic integrated circuits for compact 100^{+} Gb/s coherent optical receivers and transmitters," *IEEE J. Sel. Top. Quantum Electron.*, vol. 20, no. 4, pp. 1-8, 2014.

[19] M. J. Heck, J. F. Bauters, M. L. Davenport, J. K. Doylend, S. Jain, G. Kurczveil, S. Srinivasan, Y. Tang, and J. E. Bowers, "Hybrid silicon photonic integrated circuit technology," *IEEE J. Sel. Top. Quantum Electron.*, vol. 19, no. 4, pp. 6100117-6100117, 2013.

[20] G. H. Duan, S. Olivier, C. Jany, S. Malhouitre, A. Le Liepvre, A. Shen, X. Pommarede, G. Levaufre, N. Girard, D. Make, and G. Glastre, "Hybrid III-V Silicon Photonic Integrated Circuits for Optical Communication Applications," *IEEE J. Sel. Top. Quantum Electron.*, vol. 22, no. 6, pp. 379-389, 2016.

[21] L. Zhu, P. Chak, J. K. S. Poon, G. A. Derose, A. Yariv, and A. Scherer, "Electrically-pumped, broad-area, single-mode photonic crystal lasers," *Opt. Express*, vol. 15, no. 10, pp. 5966-5975, 2007.

[22] L. Zhu, L., G. A. Derose, A. Scherer, and A. Yariv, "Electrically-pumped, edge-emitting photonic crystal lasers with angled facets," *Opt. Lett*., vol. 32, no. 10, pp. 1256-1258, 2007.

[23] Y. Zhu, Y. Zhao, and L. Zhu, "Two-dimensional photonic crystal Bragg lasers with triangular lattice for monolithic coherent beam combining," *Sci. Rep.*, vol. 7, pp. 10610, 2017.

[24] Y. Zhao, and L. Zhu, "On-chip coherent combining of angled-grating diode lasers toward bar-scale single-mode lasers," *Opt. Express*, vol. 20, no. 6, pp. 6375-6384, 2012.

[25] L. Zhu, X. K. Sun, G. A. DeRose, A. Scherer, and A. Yariv, "Room temperature continuous wave operation of single-mode, edge-emitting photonic crystal Bragg lasers," *Opt. Express*, vol. 16, no. 2, pp. 502-506, 2008.

[26] H. Hofmann, H. Scherer, S. Deubert, M. Kamp, and A. Forchel, "Spectral and spatial single mode emission from a photonic crystal distributed feedback laser," *Appl. Phys. Lett*., vol. 90, no. 12, pp. 121135, 2007.

[27] R. J. Lang, A. G. Larsson, and J. G. Cody, "Lateral modes of broad area semiconductor lasers: Theory and experiment," *IEEE J. Quant. Elect*., vol. 27, pp. 312-320, 1991.

[28] J. P. Hohimer, G. R. Hadley, and A. Owyoung, "Mode control in broad area diode lasers by thermally induced lateral index tailoring," *Appl. Phys. Lett*., vol. 52, pp. 260-262, 1988.

[29] Y. Zhao, J. Fan, and L. Zhu, "Modal and scalability analysis of a zigzag array structure for passive coherent beam combining," *J. Opt. Soc. Am. B*, vol. 29, no. 4, pp. 650-655, 2012.

[30] W. Bogaerts, D. Taillaert, B. Luyssaert, P. Dumon, J. Van Campenhout, P. Bienstman, D. Van Thourhout, R. Baets, V. Wiaux, and S. Beckx, "Basic structures for photonic integrated circuits in silicon-on-insulator," *Opt. Express*, vol. 12, no. 8, pp. 1583-1591, 2004.

[31] D. J. Moss, R. Morandotti, A. L. Gaeta, and M. Lipson, "New CMOS-compatible platforms based on silicon nitride and Hydex for nonlinear optics," *Nat. Photonics*, vol. 7, no. 8, pp. 597-607, 2013.

[32] A. J. Zilkie, P. Seddighian, B. J. Bijlani, W. Qian, D. C. Lee, S. Fathololoumi, J. Fong, R. Shafiiha, D. Feng, B. J. Luff, and X. Zheng, "Power-efficient III-V/Silicon external cavity DBR lasers," *Opt. Express*, vol. 20, no. 21, pp. 23456-23462, 2012.

[33] A. A. Liles, K. Debnath, and L. O'Faolain, "Lithographic wavelength control of an external cavity laser with a silicon photonic crystal cavity-based resonant reflector," *Opt. Lett*., vol. 41, no. 5, pp. 894-897, 2016.

[34] A. Verdier, G. de Valicourt, R. Brenot, H. Debregeas, P. Dong, M. Earnshaw, H. Carrère, and Y. K. Chen, "Ultra-Wide Band Wavelength-Tunable Hybrid External-Cavity Lasers," *J. Lightw. Technol.*, 2017

[35] S. Romero-Garcia, B. Marzban, F. Merget, B. Shen, and J. Witzens, "Edge couplers with relaxed alignment tolerance for pick-and-place hybrid integration of III–V lasers with SOI waveguides," *IEEE J. Sel. Top. Quantum Electron.*, vol. 20, no. 4, pp.369-379, 2014.

[36] A. W. Fang, E. Lively, Y. H. Kuo, D. Liang, and J. E. Bowers, "A distributed feedback silicon evanescent laser," *Opt. Express*, vol. 16, no. 7, pp. 4413-4419, 2008.

[37] X. Sun, A. Zadok, M. J. Shearn, K. A. Diest, A. Ghaffari, H. A. Atwater, A. Scherer, and A. Yariv, "Electrically pumped hybrid evanescent Si/InGaAsP lasers," *Opt. Lett*., vol. 34, no. 9, pp. 1345–1347, 2009.

[38] S. Keyvaninia, G. Roelkens, D. Van Thourhout, C. Jany, M. Lamponi, A. Le Liepvre, F. Lelarge, D. Make, G. H. Duan, D. Bordel, and J. M. Fedeli, "Demonstration of a heterogeneously integrated III-V/SOI single wavelength tunable laser," *Opt. Express*, vol. 21, no. 3, pp. 3784-3792, 2013.

[39] X. Zheng, I. Shubin, J. H. Lee, S. Lin, Y. Luo, J. Yao, S. S. Djordjevic, J. Bovington, D. Y. Lee, H. D. Thacker, and C. Zhang, "III-V/Si hybrid laser arrays using back end of the line (BEOL) integration," *IEEE J. Sel. Top. Quantum Electrons.*, vol. 22, no. 6, pp. 204-217, 2016.

[40] T. Komljenovic, M. Davenport, J. Hulme, A. Y. Liu, C. T. Santis, A. Spott, S. Srinivasan, E. J. Stanton, C. Zhang, & J. E. Bowers, "Heterogeneous silicon photonic integrated circuits," *IEEE J. Lightw. Technol.*, vol. 34, no. 1, pp. 20-35, 2016.

[41] S. Yang, Y. Zhang, D. W. Grund, G. A. Ejzak, Y. Liu, A. Novack, D. Prather, A. E. Lim, G. Q. Lo, "Baehr-Jones, T. & Hochberg, M. A single adiabatic microring-based laser in 220 nm silicon-on-insulator," *Opt. Express.*, vol. 22, no. 1, pp. 1172-1180, 2014.

[42] T. Fan, J. P. Epping, R. M. Oldenbeuving, C. G. Roeloffzen, M. Hoekman, R. Dekker, R. G. Heideman, P. J. van der Slot, and K. J. Boller, "Optically Integrated InP-Si3N4 Hybrid Laser," *IEEE Photon. J*., vol. 8, no. 6, pp. 1-11, 2016.

[43] N. Kobayashi, K. Sato, M. Namiwaka, K. Yamamoto, S. Watanabe, T. Kita, H. Yamada, and H. Yamazaki, "Silicon photonic hybrid ring-filter external cavity wavelength tunable lasers," *J. Lightw. Technol.*, vol. 33, no. 6, pp.1241-1246, 2015.

[44] X. Luo, Y. Cheng, J. Song, T. Y. Liow, Q. J. Wang, and M. Yu, "Wafer-Scale Dies-Transfer Bonding Technology for Hybrid III/V-on-Silicon Photonic Integrated Circuit Application," *IEEE J. Sel. Top. Quantum Electrons.*, vol. 22, no. 6, pp.443-454, 2016.

[45] B. Stern, X. Ji, A. Dutt, and M. Lipson, "Compact narrow-linewidth integrated laser based on a low-loss silicon nitride ring resonator," *Opt. lett.*, vol. 42, no. 21, pp. 4541-4544, 2017.

[46] T. Komljenovic, S. Srinivasan, E. Norberg, M. Davenport, G. Fish, and J. E. Bowers, "Widely tunable narrow-linewidth monolithically integrated external-cavity semiconductor lasers," *IEEE J. Sel. Top. Quantum Electrons.*, vol. 21, no. 6, pp. 214-222, 2015.
[47] Y. Fan, R. M. Oldenbeuving, C. G. Roeloffzen, M. Hoekman, D. Geskus, R. G. Heideman, and K. J. Boller, "290 Hz intrinsic linewidth from an integrated optical chip-based widely tunable InP-Si3N4 hybrid laser," *CLEO: A&T.*, San Jose, CA, 2017.
[48] G. de Valicourt, C. M. Chang, M. S. Eggleston, A. Melikyan, C. Zhu, J. Lee, J. E. Simsarian, S. Chandrasekhar, J. H. Sinsky, P. Dong, and K. Kim, "Photonic integrated circuit based on Hybrid III-V/Silicon Integration," *J. Lightw. Technol*., 2017.
[49] T. Y. Fan, "Laser beam combining for high-power, high-radiance sources," *IEEE J. Sel. Top. Quantum Electron*., vol. 11, pp. 567–577, 2005.
[50] Y. Zhu, Y. Zhao, and L. Zhu, "Loss induced coherent combining in InP-Si3N4 hybrid platform," *Sci. Rep*., vol. 8, pp. 878, 2018.
[51] M. Khajavikhan, and J. R. Leger, "Modal analysis of path length sensitivity in superposition architectures for coherent laser beam combining," *IEEE J. Sel. Top. Quantum Electron*., vol. 15, no. 2, pp. 281-290, 2009.
[52] K. Schires, N. Girard, G. Baili, G. H. Duan, S. Gomez, and F. Grillot, "Dynamics of Hybrid III-V Silicon Semiconductor Lasers for Integrated Photonics," *IEEE J. Sel. Top. Quantum Electron.*, vol. 22, no. 6, pp. 43-49, 2016.
[53] L. Zhu, "Photonic crystal Bragg lasers: design, fabrication, and characterization," Ph.D. dissertation, Caltech, CA, USA, 2008.
[54] K. Kobayashi, and I. K. U. O. Mito, "Single frequency and tunable laser diodes," *J. Lightw. Technol.*, vol. 6, no. 11, pp. 1623-1633, 1988.
[55] A. J. Ward, D. J. Robbins, G. Busico, E. Barton, L. Ponnampalam, J. P. Duck, N. D. Whitbread, P. J. Williams, D. C. Reid, A. C. Carter, and M. J. Wale, "Widely tunable DS-DBR laser with monolithically integrated SOA: design and performance," *IEEE J. Sel. Topics Quantum Electron*., vol. 11, no. 1, pp. 149–156, Jan. 2005.